MADRID
inter.noise 2019
June 16 - 19
NOISE CONTROL FOR A BETTER ENVIRONMENT

Experimental Investigation of an Under-expanded Single Stream Jet Interacting with a Tangential Flat Plate: Flow Visualizations and Wall Pressure Statistics

R. Camussi [1]
S. Meloni [2]
E. de Paola [3]
M. Khalil [4]
A. Di Marco [5]
A. Fagotto[6]

Università Roma Tre, Dipartimento di Ingegneria
Via della Vasca Navale 79, 00146 Roma (Italy)

ABSTRACT

This paper is devoted to the experimental study of a circular converging nozzle in under-expanded conditions interacting with a tangential flat plate. Measurements were carried out in the semi-anechoic chamber of the Fluid Dynamic laboratory at the University Roma Tre. Wall pressure fluctuations are acquired by means of flush mounted Kulite sensors displaced at several streamwise positions. Qualitative flow visualizations are obtained as well, through the Background Oriented Schlieren technique that provides density gradient fields integrated along the optical path. A parametric study is carried out in terms of jet/plate distance and nozzle pressure ratio. The investigation provides, for the first time, a detailed characterization of the wall pressure statistics also correlating the achieved statistics with the shock cell structure.

Keywords: Under-expanded Jet, Wall Pressure Statistics, Tangential Flat Plate Interaction, Background Oriented Schlieren

[1] roberto.camussi@uniroma3.it
[2] stefano.meloni@uniroma3.it
[3] elisa.depaola@uniroma3.it
[4] mohsin.ahmad@uniroma3.it
[5] alessandro.dimarco@uniroma3.it
[6] andrea.fagotto92@gmail.com

1. INTRODUCTION

The interaction between engine exhaust flow and the aircraft structural parts represent one of the main problems of the installation of modern Ultra High Bypass Ratio engines. A commercial aircraft in cruise condition is typically at speed of the order of $M_f = 0.8$ and the flight altitude is usually around 11000m. Due to this flight conditions and the thrust requirements, the nozzle exhaust flow is generally supersonic and imperfectly expanded[1]. Therefore, in addition to subsonic noise sources there are a series of expansion and compression waves which interact with the aircraft structures increasing the panels stress and the cabin noise which adds to passenger discomfort as well.

Due to the importance of the installation effects of modern turbofan engines, the influence of solid surfaces located in the vicinity of the jet flow on the surrounding pressure field, has been the subject of several investigations [2–7] that included the analysis of shielding and scattering effects[8] and different nozzle geometries. Recent studies were also devoted to the analysis of wall pressure fluctuations induced by jets over a tangential flat plate[9–11]. The latter investigations were focused on incompressible and subsonic jet flows. The aim of the present research study is to extend those analyses to under-expanded jets, a scheme that closely mimics real flight configurations. Many research studies have been carried out to study the acoustic signature of under-expanded free jets in different flow conditions[12–18]. It has been found that the interaction between the downstream travelling flow structures and shock cells is the source of shock-associated noise[13] whereas the screech is a result of a feedback loop mechanism. However, the wall pressure field induced by under-expanded jets has never been studied so far and the present work contributes to clarify this issue.

In the present approach, wall pressure data are measured using flush mounted transducers and flow visualizations is carried out using the Background Oriented Schlieren (BOS) technique. The wall pressure measurements are carried out at different axial positions along the flat plate in the streamwise direction whereas the radial distance H between the nozzle and the flat plate is varied between H/D=0.75 and H/D=2, where D is the nozzle exhaust diameter. According to previous investigations[18] the selected range of H/D is of interest because of the presence of three different zones characterizing the jet-wall interaction: a free jet shear layer close to the nozzle exit, a shear layer-wall boundary layer interaction zone at intermediate distances, and a fully developed turbulent wall boundary layer zone very far from the nozzle exit. It is of interest to analyze the characteristics of these zones when the jet is under-expanded.

The analyzed configurations span from exit Mach number M_j=0.9 up to M_j=1 and to a maximum Nozzle Pressure Ratio NPR= 1.94 that is close to a typical situation encountered in real engines. Wall pressure data are analyzed using the Fourier transform as well as through the Wavelet decomposition that provides a time-frequency representation of the signals.

Details about the experimental setup and the procedure adopted to carry out the experiments are presented in the next section. Section 3 reports the main results in terms of flow visualizations, classical Fourier-based spectral analysis and time-frequency decompositions. Final remarks and conclusions are given in the last section.

2. EXPERIMENTAL SETUP AND PROCEDURES

2.1. Facility

Measurements have been performed at University of Roma Tre in the Laboratory of Fluid Dynamics “G. Guj”. The jet facility is installed in a semi-anechoic chamber that measures 2 m *x* 4 m *x* 3m and equipped with sound absorbing 10cm lengthy foam panels

backed with wooden insulation. This installation provides semi-anechoic conditions for frequencies above 500 Hz. The nozzle is connected to an air duct through a pressure regulator and a muffler. Compressed air is supplied from a $2m^3$ air tank at 8bar delivering continuous dry air that goes through an 80mm diameter plenum, equipped with mesh screens and a honeycomb. The electronically controlled valve maintains the nozzle pressure ratio to within 1% of the desired set point. A rigid flat plate has been placed parallel to the nozzle axis. The alignment of the flat plate has been carefully checked using a laser levelling instrument. The converging nozzle has a contoured shape and an outlet diameter of D=12 mm. Jet Mach numbers spanning from 0.9 to 1 have been investigated in details including slightly under expanded conditions up to NPR=1.94 (Nozzle Pressure Ratio) which is the target condition according to real engines situations. Measurements have been carried out considering free jet condition and radial distances (H) of the plate from the centerline equal to H/D=2, H/D=1.5 and H/D=0.75

2.2. Wall Pressure Measurements Setup

The flat plate was pre-drilled with 200 taps whose spacing distances in the stream-wise and span-wise directions are equal to the jet exhaust diameter. The frame of reference for an easier visualization is reported at the corner of the plate, but it should be considered as centered on the jet axis at the nozzle exhaust. The jet flat plate setup is shown in Figure 1.

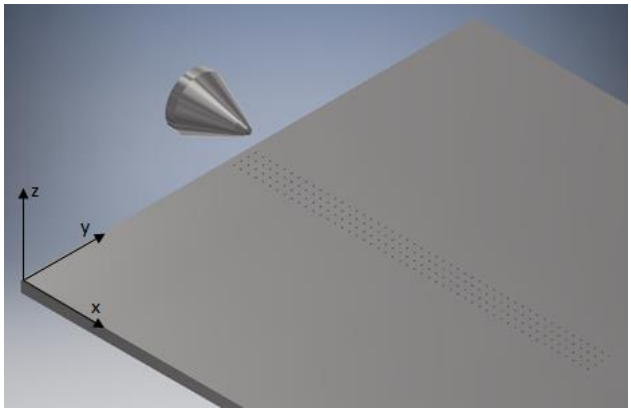

Figure 1: Wall Pressure Measurement Setup

The wall pressure fluctuations were acquired using flush mounted pressure transducers (Kulite Mic190M) with a diameter that fits the pressure taps and a frequency response of 100kHz that corresponds to the mechanical resonant frequency. The pressure transducers were connected at a signal conditioner where the cut-off filter was set at 70kHz. The signals were acquired by a digital scope Yokogawa DL708E with a sampling frequency of 200kHz, that respects the Nyquist-Shannon theorem, and for an acquisition time of 10s.

2.3. Flow Visualization Setup

Non-intrusive flow measurement techniques are gaining popularity in the recent times and advancement of the scientific cameras made a new breakthrough into the flow measurement techniques. One of such techniques is the Background Oriented Schlieren (BOS), the principle being the refractive index variation due to density gradients.

First, a reference image is generated by recording the background pattern observed through air at rest before the experiment. In the second step, an additional exposure through the flow under investigation leads to a locally displaced image of the background

pattern. The resulting images of both exposures can then be evaluated by image correlation methods. Existing evaluation algorithms, which have been developed and optimized, for example, for particle image velocimetry can then be used to determine the displacement of patterns at multiple locations throughout the image. The deflection of a single beam contains information about the spatial gradient of the refractive index integrated along the line of sight[19]

In the present study a structured pattern background is created using MATLAB program generating a 2000x2000 size matrix of random numbers whose elements are normally distributed and then printed out as a binary image of white dots. The size of the recorded dots dimension is kept about 2-3 pixels[20]. The CCD camera used for the measurements is a LaVision SX 4M with a resolution of 2360x1776 pixels and equipped with Nikon auto-focus lens characterized by a focal length of 50 mm. Recording frequency has been set to 10Hz.

The pattern has been uniformly back-illuminated by a white LED screen. To determine the background image displacements a particle image velocimetry (PIV) cross-correlation algorithm has been applied using the Davis software provided by LaVision. Interrogation window has been set at constant size corresponding to 16x16 pixels with a 50% overlap. Tests have been performed by placing the camera and the back-illuminated pattern at the same distance from the nozzle axis as shown in Figure 2. The frame of reference is also reported in the same figure. For all test cases 200 images were acquired.

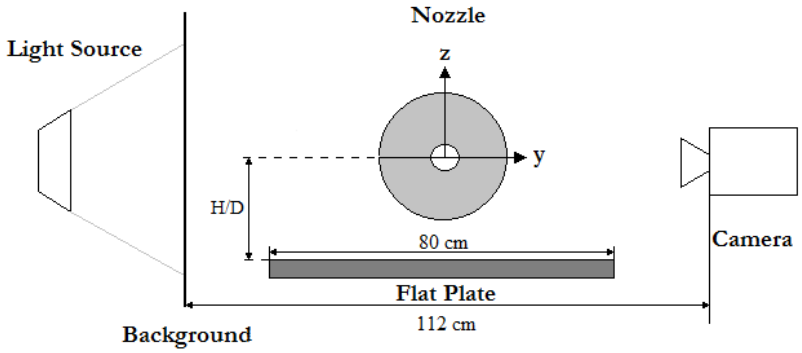

Figure 2: BOS Visualization Setup

3. RESULTS

An example of a BOS visualization obtained at NPR=1.94, H/D = 2 is reported in Figure 3. From the flow visualization in Figure 3 it is evaluated the lengths of the shock cells as the distance between two consecutive peaks of the pixel displacement trend along the jet axis. For a clearer visualization the divergence of the pixel displacement has been considered and the resultant of Shock Cell Length has been averaged over the entire shock cell train assuming a constant spacing between two shock cells for a preliminary evaluation.

(a) (b)

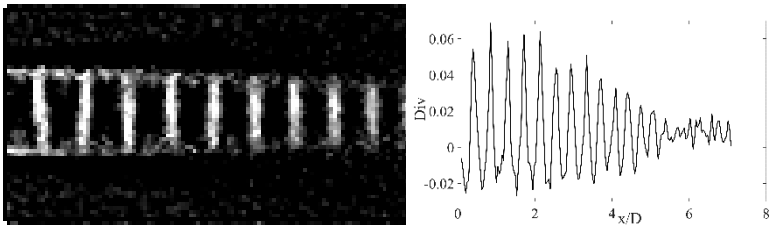

Figure 3: (a)Background Oriented Schlieren Flow Visualization at NPR = 1.94, H/D = 2. (b) Axial evolution of Divergence of pixel displacement at jet centerline at NPR = 1.94, H/D = 2

The achieved shock cell length is compared against the model provided by Harper-Bourne and Fisher[21] as well as model provided by Prandtl and Packs[22]. Considering these different shock cell lengths, the shock cell frequency peaks has been computed, using the Equation 1.

$$f_P = \frac{U_{conv}}{L_{SC}(1-M_{conv}\cos\theta)} \tag{1}$$

Where, U_{conv} is convection velocity, L_{SC} is shock cell length evaluated from flow visualization or theorical model and M_{conv} is the convection Mach number defined as $M_{conv} = \frac{U_{conv}}{c_\infty}$, where c_∞ is freestream sound velocity and θ is the angle with respect to the nozzle axis . In order to compare these results with the frequency peak evaluated with the flush mounted pressure transducers over the plate surface we have assumed $\theta = 90°$. The convection velocity is computed according to a classical estimation commonly used in the literature[23], that is:

$$U_{conv} = 0.6U_j \tag{2}$$

The associated Strouhal number St_p has been estimated using the following equation:

$$St_P = \frac{f_p \cdot D}{U_j} \tag{3}$$

where U_{jet} is the jet exhaust velocity and f_p is shock cell peak frequency associated to the Broad Band Shock Associated Noise (BBSAN). Table 1 reports a comparison of the present experimental results and the theoretical models

Table 1: Comparison between theoretical and experimental evaluation of BBSAN Strouhal Numbers

	Experimental	Harper-Bourne & Fisher	Prandtl & Packs
St_P	1,5365	1,6431	1,395

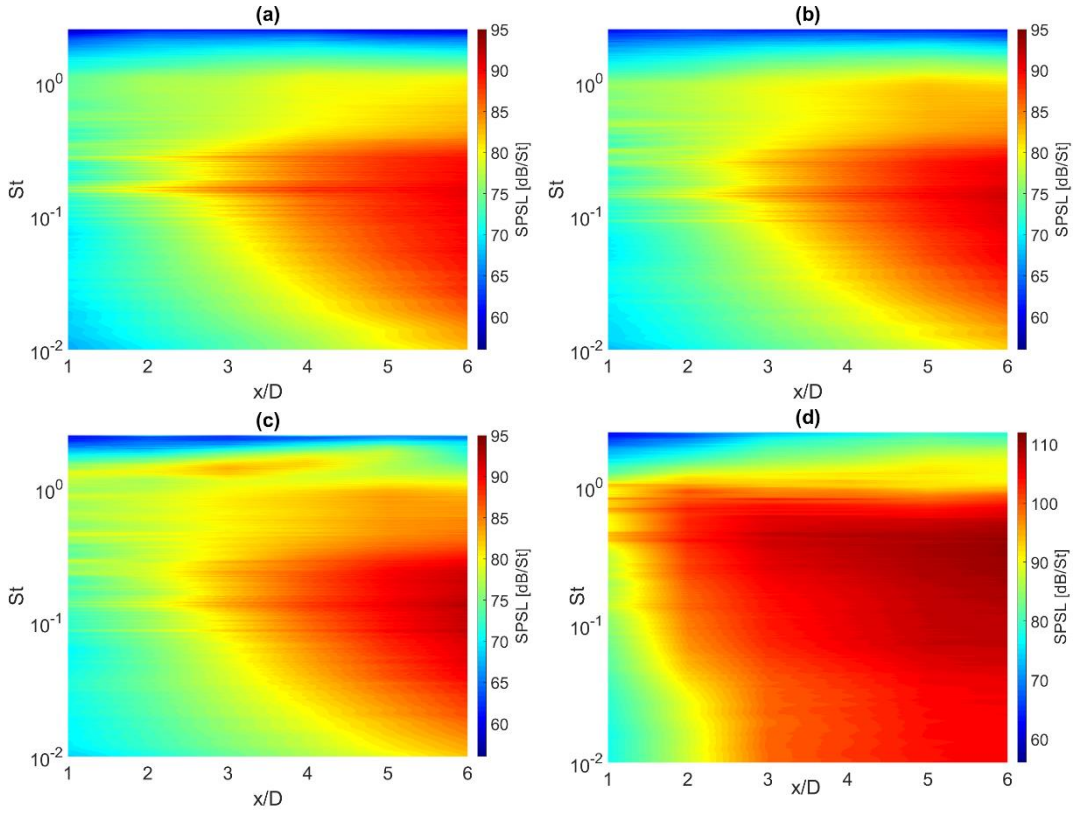

Figure 4: (a) SPSL Wall Pressure Map at H/D=2, NPR=1.70, (b) H/D=2, NPR=1.84, (c) H/D=2, NPR=1.94, (d)H/D=0.75, NPR=1.94

The uni-variate statistics are analyzed in frequency domain using the Power Spectral Density (PSD) evaluated with the Welch method. Spectra are presented in terms of Sound Pressure Spectrum Level (SPSL) [24] in dB/St, St being based on the nozzle exhaust velocity and the jet diameter, as reported in the following:

$$SPSL = 10\log_{10}\left(\frac{PSD}{P_{ref}^2}\frac{U_j}{D}\right) \tag{4}$$

where Δf_{ref}= 1Hz and P_{ref}= 20μPa. Figure 4 reports the SPSL as a function of St and x/D for different NPR and H/D. It can be observed that for the whole set of conditions considered, the largest amplitudes are reached at the end of the potential core, that is for x/D between 5 and 6. The increase of the NPR does not affect this behavior except for the onset of an energy bump at high frequencies corresponding to St > 1. This behavior is a signature of the BBSAN. A reduction of the distance from the plate, that is for H/D = 0.75, leads to an amplification of the hydrodynamic effects leading to a relevant increase of broadband energy whereas the BBSAN trace disappears. Indeed, in this configuration the impact point of the jet above the flat plate is at about x/D=3.5.
The two points statistical analysis was carried out in the frequency domain by evaluating the coherence function according to the definition given below [25].

$$\gamma(\xi,\omega) = \frac{|\varphi_{p1p2}(\xi,\omega)|}{[\varphi_{p1}(\omega)\varphi_{p2}(\omega)]^{1/2}} \tag{5}$$

where ω is the angular frequency, $\varphi_{p1p2}(\xi,\omega)$ is the cross-spectrum, $\varphi_{p1}(\omega)$ and $\varphi_{p2}(\omega)$ the auto-spectra of two consecutive transducers separated in the streamwise

direction by $\xi = 1D$. The coherence spectra versus the normalized angular frequency $\frac{\omega\xi}{U_c}$ and $\gamma(\xi,\omega)$[26] are reported in Figure 5 for the same flow conditions of Figure 4.

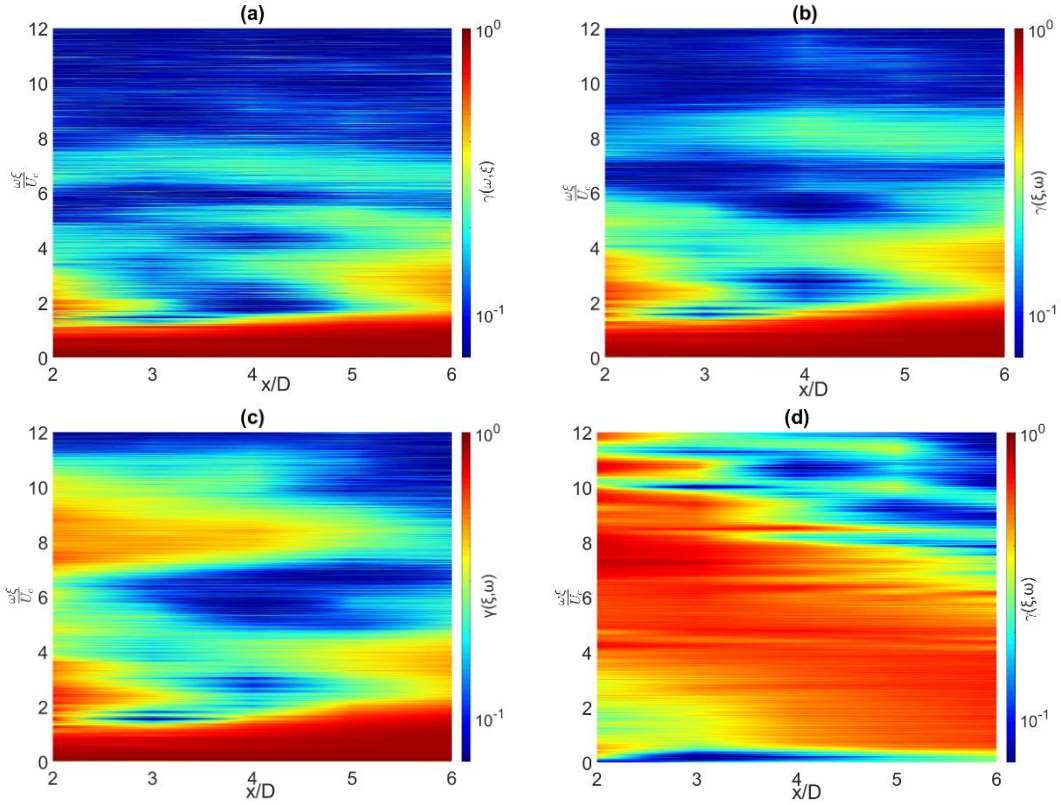

Figure 5: Coherence Map at (a)H/D=2, NPR=1.70, (b)H/D=2, NPR1.84, (c)H/D=2, NPR=1.94, (d)H/D=0.75, NPR=1.94

For the H/D=2 cases (a-b-c), the coherence function exhibits the expected bump at very low frequencies, a behavior that is further enhanced by increasing M. In the under-expanded condition (case c) another pressure event is visualized around $\frac{\omega\xi}{U_c} = 8$. This effect can be ascribed to BBSAN since, according to the previous results, it is evident at small axial positions and disappears at the end of the potential core. When the plate is very close to the jet (case d) the bump at very low frequencies disappears as well as the clear signature of the BBSAN. In this configuration the wall pressure fluctuations are dominated by hydrodynamic component and the spectra content is much more complex.

In order to provide a more accurate estimation and characterization of the BBSAN, the wall pressure fluctuations are analyzed using a continuous wavelet transform (CWT), the formulation being presented in the following equation:

$$w(s,t) = C_{\psi}^{-1/2} s^{1/2} \int_{-\infty}^{+\infty} p(\tau)\psi^*(\tfrac{t-\tau}{s})d\tau \qquad (6)$$

where $C_{\psi}^{-1/2}$ is a constant that takes into account the mean value of $\Psi\ (t)$ and $\psi^*(\frac{t-\tau}{s})$ is the complex conjugate of the dilated and translated mother wavelet $\Psi\ (t)$. Therefore, the wavelet transform consists in a convolution of a temporal signal with a dilated and translated function with different scales of dilatation.

The CWT was computed using a complex bump wavelet kernel defined in the literature [27] [28]. A window of 4096 samples has been adopted and the results are averaged

on 200 windows to provides more clear statistics. Figure 6 reports a segment of the time-frequency wavelet scalogram that, according to the previous spectral results, enhances the energy contained around St=1 and the different behavior observed for H/D=0.75 (case d).

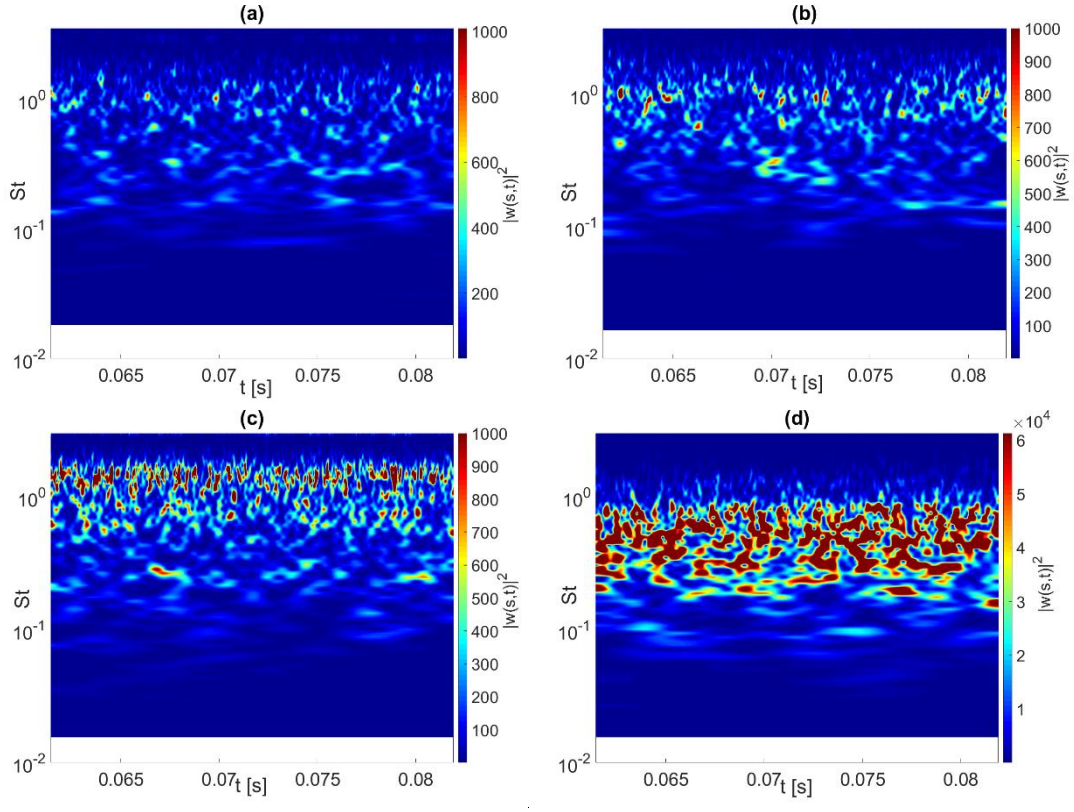

Figure 6: (a)Square of wavelet coefficients at H/D=2, x/D=3, NPR=1.70, (b)H/D=2, x/D=3, NPR=1.84, (c)H/D=2, x/D=3, NPR=1.94, (d)H/D=0.75, x/D=3, NPR=1.94

As pointed out by M. Farge[29], the Fourier spectra can be recovered by integrating the wavelet scalogram in time, this procedure providing spectra less affected by statistical uncertainties. The pressure maps are reported in Figure 7 for different NPR. The use of the wavelet-based procedure provides a clear visualization of the potential core effect that leads to an increase of the energy content at about x/D>5 and for St around 0.3, the typical frequency of the Kelvin-Helmholtz instability of the jet shear layer. When H/D decreases, this trace is still present but at slightly higher St. In the under-expanded condition (case c) the signature of the BBSAN is now very clearly visible for St>1 showing the classical banana shape found in the literature[30]

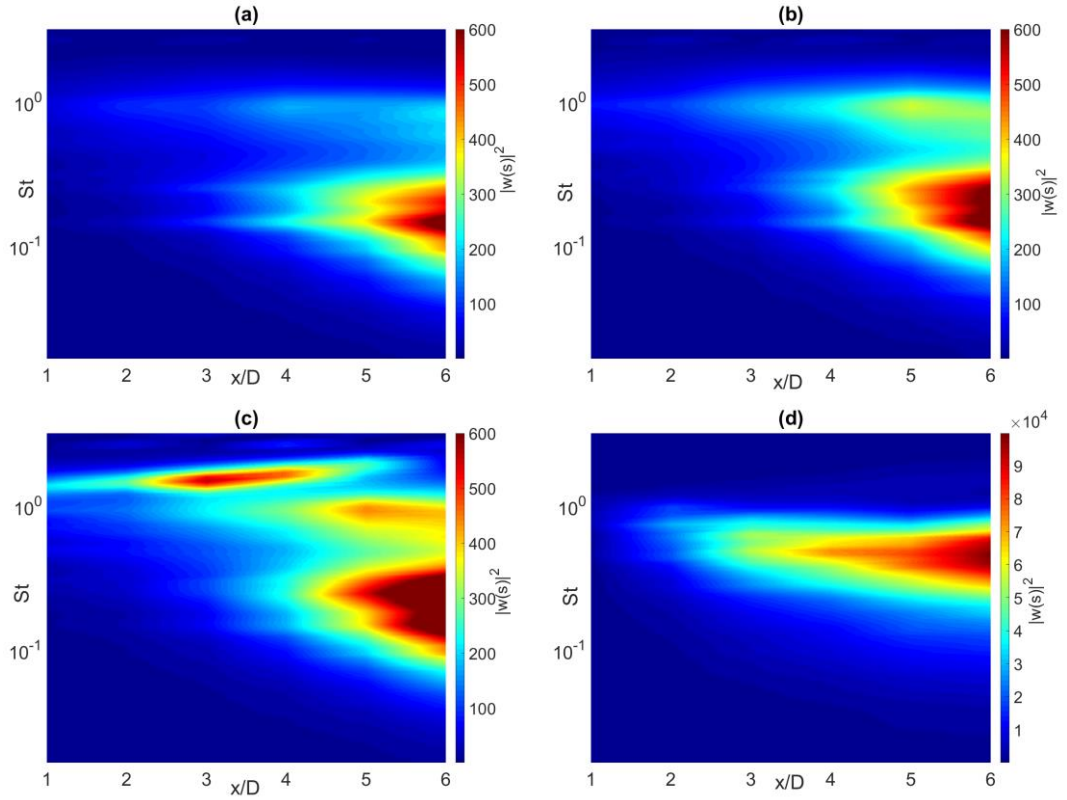

Figure 7: (a)Square of Wavelet coefficients in the frequency domain at H/D=2, NPR=1.70, (b)H/D=2, NPR=1.84, (c)H/D=2, NPR=1.94, (d)H/D=0.75, NPR=1.94

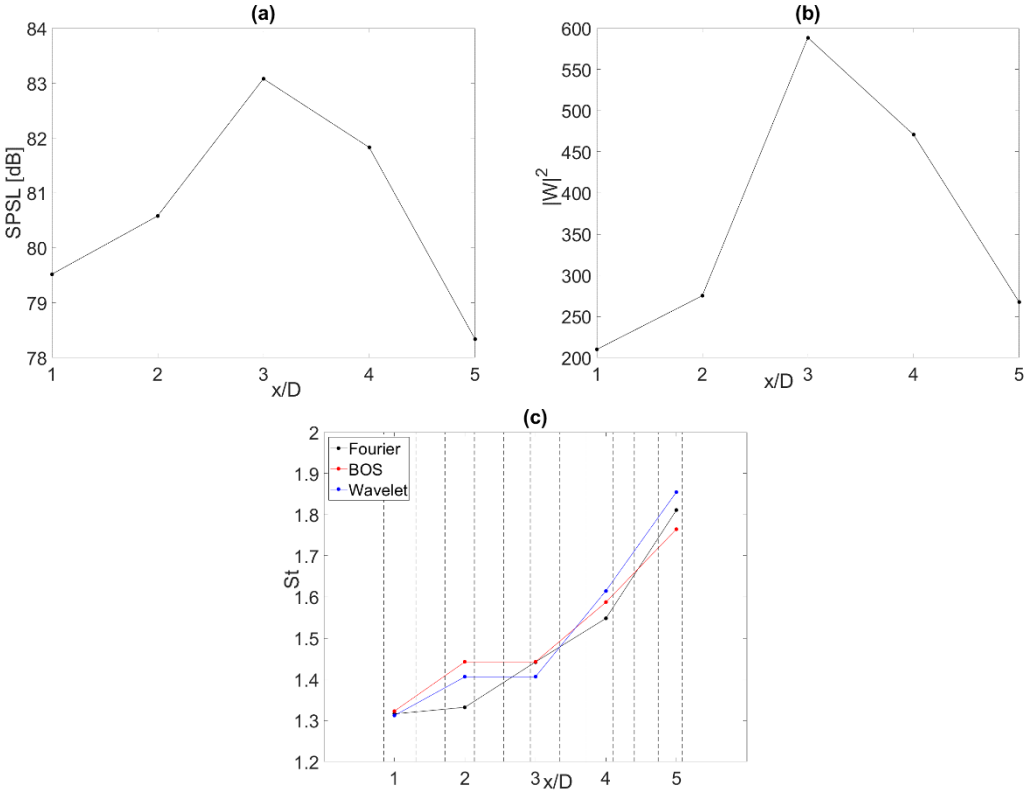

Figure 8: (a)Axial Evolution of BBSAN amplitude using Fourier at H/D=2, NPR=1.94, (b)Axial Evolution of BBSAN peak using Wavelet at H/D=2, NPR=1.94, (c)Strouhal number comparison using Fourier, BOS and Wavelet analysis

In Figure 8, It is possible to observe that the estimation provided by the three methods are very similar to each other. Cases a) and b) report the estimation obtained in the Fourier and Wavelet domain respectively. Both methods indicate that the largest energy associated to the BBSAN is at about x/D=3. The comparison among the Strouhal numbers is instead reported in Figure 8c showing a good agreement and the expected trend due to the increase of the shock cell separation for increasing x/D.

4. CONCLUSION

This paper presents an analysis of the wall pressure fluctuations induced by a single stream jet around the sonic conditions. The wall pressure measurements are carried out using flush mounted pressure transducers varying the Nozzle Pressure Ratio (NPR) = 1.70 to NPR = 1.94 and flat plate radial position from H/D = 0.75 to H/D = 2. Wall pressure analysis was combined along with flow visualizations using Background Oriented Schlieren (BOS) technique.

This research study presents following findings:

- Shock Cell Length (SCL) is calculated using BOS technique. The achieved shock cell length is compared against the model provided by Harper-Bourne and Fisher[21] as well as by Prandtl and Packs[22].
- Broad Band Shock Associated Noise (BBSAN) Strouhal number is calculated and compared with the Strouhal number computed using above mentioned models and a quite good agreement is observed.
- The Fourier spectrum and Wavelet coefficients calculated with bump kernel are used to analyze the signal in time and frequency domain. Both SPSL and Wavelet coefficients show a signature at about St = 1, at H/D = 2 and NPR = 1.94, which is indication of Broad Band Shock Associated Noise (BBSAN).
- This signature disappears in the close coupled configuration, e.g. H/D = 0.75 and NPR = 1.94.

Further investigations are needed in order to understand the role of screech tones one the wall pressure fluctuations. To study this, a new series of experiments is under process.

5. REFERENCES

1. Huber J. Fleury V. Bulté J. Laurendeau E. & Sylla A. A. *"Understanding and Reduction of Cruise Jet Noise at Aircraft Level"*. *Int. J. Aeroacoustics* **13**, 61–84 (2014).
2. André B. Castelain T. & Bailly C. *"Broadband Shock-Associated Noise in Screeching and Non-Screeching Underexpanded Supersonic Jets"*. AIAA Journal, Vol. 51, No. 3 , pp. 665-673. (2013) doi:10.2514/1.J052058
3. Schram C. F. "*Aeroacoustics of Subsonic Jets: Prediction of the Sound Produced by Vortex Pairing based on Particle Image Velocimetry"*. Eindhoven: Technische Universiteit Eindhoven (2003). doi:10.6100/IR561402
4. Mercier B. Castelain T. & Bailly C. *"Experimental characterisation of the screech feedback loop in underexpanded round jets"*. J. Fluid Mech. 824, 202–229 (2017). doi:10.1017/jfm.2017.336
5. Nakazono Y. Aoki S. & Saguanrum S. "*Near-Field Acoustic Characteristics of Underexpanded Jets from Notched Nozzles*". Journal of JSEM, Vol.11, Special Issue (2011) SS47-SS52
6. Yerapotina S. *"Aeroacoustic Characteristics of Supersonic Twin Jets"*. *Florida State Univ. Libr.*. Florida State University Libraries, (2005)
7. Morris P. J. & Zaman K. B. M. Q. *"Velocity measurements in jets with application to noise source modeling. " J. Sound Vib.* **329**, 394–414 (2010). doi.org/10.1016/j.jsv.2009.09.024
8. André B. Castelain T. & Bailly C. "*Experimental exploration of an underexpanded supersonic jet*. " 28th International Symposium on Shock Waves pp 629-634
9. Miller S. A. E. & Morris P. J. "*The Prediction of Broadband Shock-Associated Noise Including Propagation Effects*." International Journal of Aeroacoustics, December 1, 2012,Vol 11, Issue 7-8, 2012. doi.org/10.1260/1475-472X.11.7-8.755
10. Brown C. A. Podboy G. G. & Bridges J. E. *"Modeling Jet-Surface Interaction Noise for Separate Flow Nozzles"*. in 22nd AIAA/CEAS Aeroacoustics Conference (American Institute of Aeronautics and Astronautics, 2016). doi:10.2514/6.2016-2862
11. da Silva F. D. da Silva A. R. Deschamps C. J. Jordan P. Piantanida S. Cavalieri A. V. and Brès G. A.. *"Effects of coherence on jet-surface interaction noise"*. in 22nd AIAA/CEAS Aeroacoustics Conference (American Institute of Aeronautics and Astronautics, 2016). doi:10.2514/6.2016-2860
12. Piantanida S. Jaunet V. Huber J. Wolf W.R. Jordan P. Cavalieri A. V. *"Scattering of turbulent-jet wavepackets by a swept trailing edge"*. *J. Acoust. Soc. Am.* **140**, 4350–4359 (2016).
13. Mancinelli M. Di Marco A. Camussi R., *"Multivariate and conditioned statistics of velocity and wall pressure fluctuations induced by a jet interacting with a flat plate"*. J. Fluid Mech **823**, 247–272 (2018). doi:10.1017/jfm.2017.307
14. Smith M. J. Miller S. A. *"The Effects of Surfaces on the Aerodynamics and Acoustics of Jet Flows"*. 19th AIAA/CEAS Aeroacoustics Conf. 1–21 (2013). doi:10.2514/6.2013-2041
15. Meloni S. Di Marco A. Mancinelli M. & Camussi R. *FIV2018-154* "*Reynolds Number Effect On Wall Pressure Fluctuations Induced By A SubsonicJet On A Tangential Flat Plate*. "(2018)
16. André B. Castelain T. and Bailly C. "*Experimental study of flight effects on underexpanded supersonic jet noise*. " (2013).19th AIAA/CEAS Aeroacoustics

Conference, doi: 10.2514/6.2013-2079
17. Meloni S. Di Marco A. Mancinelli M. Camussi R. *"Wall pressure fluctuations induced by a compressible jet flow over a flat plate at different Mach numbers".* Exp Fluids (2019) 60: 48. doi.org/10.1007/s00348-019-2696-3
18. Di Marco A. Mancinelli M. Camussi R. "*Pressure and velocity measurements of an incompressible moderate Reynolds number jet interacting with a tangential flat plate*". J. Fluid Mech **770**, 247–272 (2018).
19. Vinnichenko, N. A., Uvarov, A. V & Plaksina, Y. Y. "*Accuracy of background oriented schlieren for different background patterns and means of refraction index reconstruction*. "
20. De Paola E. Di Marco A. Meloni S. Camussi R. "*Density measurements of a compressible jet flow interacting with a tangential flat plate using Background-Oriented Schlieren*". ITI 2018
21. Harper-Bourne M. & Fisher M. J. "*The Noise from Shock Waves in Supersonic Jets*". *AGARD Conf. Noise Mech.* 1–13 (1973).
22. Pack d. C. "A note on prandtl's formula for the wave-length of a supersonic gas jet". *Q. J. Mech. Appl. Math.* **3**, 173–181 (1950).
23. Tinney C. E. & Jordan P. *"The near pressure field of co-axial subsonic jets. J. Fluid Mech.* **611**, 175–204 (2008).
24. Pierce A. D. Smith P. W. "*Acoustics: An Introduction to Its Physical Principles and Applications*". *Phys. Today* **34**, 56–57 (1981).
25. Di Marco A. Camussi R. Bernardini M. Pirozzoli S. "*Wall pressure coherence in supersonic turbulent boundary layers*". *J. Fluid Mech.* **732**, 445–456 (2013).
26. Farabee T. M. & Casarella M. J. *"Spectral features of wall pressure fluctuations beneath turbulent boundary layers. "* Phys. Fluids A Fluid Dyn. **3**, 2410–2420 (1991).
27. Jiang Q. & Suter B. W. "*Instantaneous frequency estimation based on synchrosqueezing wavelet transform*". *Signal Processing* **138**, 167–181 (2017).
28. Mancinelli M. Jaunet V. Jordan P. & Towne, "*A. Screech-tone prediction using upstream-travelling jet modes*". Exp. Fluids **60**, 22 (2019).
29. Farge M. "*Wavelet Transforms and their Applications to Turbulence*". *Annu. Rev. Fluid Mech.* **24**, 395–458 (1992).
30. Savarese A. Jordan P. Girard S. Royer A. & Fourment C. *"Experimental study of shock-cell noise in underexpanded supersonic jets".* AIAA Journal ,1–15 (2013).